
**Fig. 1.** A 54-year-old man had spontaneous rupture of the right gastric artery. **a** Arterial phase computed tomography (CT) shows intraperitoneal hemorrhage and extravasation of contrast material from the right gastric artery (*arrow*). **b** Celiac arteriography shows the tortuous right gastric artery with aneurysmal dilatation (*arrow*). **c** Arteriography of the right gastric artery raises a suspicion of segmental arterial mediolysis. **d** Right gastric artery was embolized using 32 Tornado Coils through a 1.8F tip microcatheter. **e** Celiac arteriography after microcoil embolization shows occlusion of the right gastric artery. Hemostasis was obtained with the procedure

migrated into the right hepatic artery), and additional coil embolization of the gastroduodenal artery stump was attempted because of recurrent bleeding. After coil migration, the microcatheter was exchanged for a 2.2F tip Progreat $\beta^3$ microcatheter (Terumo), and coil embolization of the gastroduodenal stump was performed using a 5 cm long Liquid Coil. The distal part of the Liquid Coil also partially migrated into the right hepatic artery. Subsequently, the dorsal pancreatic artery derived from the superior mesenteric artery was embolized using Liquid Coils though a Masters Parkway microcatheter. The bleeding stopped after the procedure (Fig. 2).

## Discussion

Microcoils are widely used for arterial embolization, and they are effective for localized and permanent vascular occlusion.[1,2,4–6] Several microcoil designs have been developed and used for abdominal vascular interventional procedures.[4–6] Coil embolization for gastrointestinal bleeding and traumatic vascular lesions is an alternative to surgery.[1]

A thinner microcatheter has an advantage over a conventional microcatheter for highly selective catheterization,[3] and it is mainly used for TACE for HCCs. Combined use of coil embolization during the procedure makes it possible to perform effective TACE through unselectable tumor-feeding branches.[2] In addition, coil embolization of nonhepatic branches originating from the hepatic arteries or arterioportal shunts in the tumor-bearing area may reduce the adverse effects of TACE. Coil embolization is frequently necessary during TACE for HCC. However, coil deployment is not accepted by most thinner microcatheters because of the narrow inner lumens. Therefore, another microcatheter with a wider lumen is required to perform microcoil embolization. If microcoils can be deployed through thinner microcatheters, it may reduce the cost. In addition, treatment outcomes may become safer and more effective when embolization is performed as selectively as possible. To keep the embolized vessels to a minimum, the ischemic tissue damage in the embolized vascular territory may be reduced. From such viewpoints, we proposed to deploy microcoils through thinner microcatheters.

According to the instructions on how to use the Tornado Coil, the coils are recommended for use through microcatheters that accept 0.018-inch maximum diameter guidewires. In the present study, we used four types of microcatheter with a tip of 2F or less. According to product information for each of these thinner microcatheters, one microcatheter (Masters Parkway) can accept only a 0.018-inch guidewire. Two microcatheters (Progreat α and Carnelian Pixie) accept a 0.016-inch guidewire, and one microcatheter (Carry Win) accepts only a 0.014-inch guidewire. The minimal inner diameter of each microcatheter is 0.017-inch (Carnelian Pixie and Carry Win), 0.019-inch (Progreat α), and 0.022-inch (Masters Parkway), respectively. However, our personal experience is that a 0.017-inch pusher wire can be passed through a microcatheter (Carry Win) that accepts a 0.014-inch guidewire. We speculate that the true inner

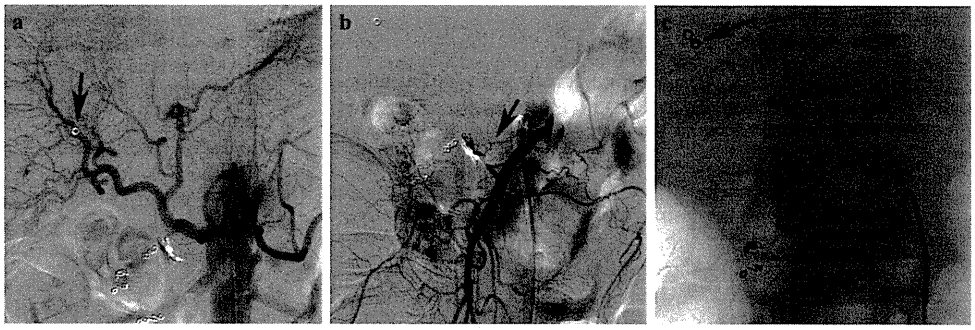


**Fig. 2.** A 59-year-old woman had recurrent bleeding from pancreatic carcinoma after coil embolization. **a** Celiac arteriography shows that the gastroduodenal artery had been embolized by microcoils at another hospital. The migrated coil in the right hepatic artery was also seen (*arrow*). **b** Superior mesenteric arteriography shows the patent dorsal pancreatic artery (*arrow*). **c** One Tornado Coil was delivered into the gastroduodenal artery stump through a 2F tip microcatheter, but it migrated into the right hepatic artery (*arrow*). The microcatheter was exchanged for a 2.2F tip microcatheter, and one 5 cm long Liquid Coil was delivered. The distal part of the Liquid Coil partially migrated into the right hepatic artery (*arrowhead*). Subsequently, the dorsal pancreatic artery was embolized using two Liquid Coils through a 2F tip microcatheter (*asterisk*). Hemostasis was successful and was maintained until the patient's death 3 months later

diameter of each thin microcatheter may be wider than that described in the specifications.

Both the Liquid Coils and Tornado Coils could be deployed through all four types of thinner microcatheter, and there were no coil jams in the catheter during any procedure in this series. In one case, 32 Tornado Coils were deployed through a microcatheter that accepted only a 0.014-inch guidewire without difficulty. Our results indicated that thinner microcatheters had a sufficient lumen to deploy Liquid Coils and Tornado Coils. In addition, a 0.016-inch GT-wire could be used as a pusher-wire to deliver the Tornado Coils. We believe that superselective coil embolization through a thinner microcatheter may improve the technical success and expand the indications for abdominal vascular interventional procedures as well as reduce the cost.

Coil migration occurred with one Tornado Coil (0.3%) deployed into the gastroduodenal artery stump. In this case, two causes of coil migration were speculated. First, the gastroduodenal artery stump was too short to place the Tornado Coil. Second, the microcatheter tip was too flexible and could not be stabilized because it was not deeply advanced into the gastroduodenal artery. In such a case, we do not recommend the use of a thinner microcatheter to deploy the microcoils. Detachable microcoils may be safe and effective, although they are expensive and a special microcatheter is required.

There are several limitations in this study. First, we used only two types of microcoil. Our results did not support the passage of other types. In an experimental study by Tajima et al.,[7] other types of microcoils [Hilal (Cook), Micronester (Cook), Vortex (Boston Scientific), and C-Stopper Coil (Piolax)] could be passed through a 2F tip microcatheter (Meister Cath Superselective Plus; Medikit, Tokyo, Japan) using a saline-flush technique. However, we have never deployed microcoils other than Liquid Coils and Tornado Coils through a thinner microcatheter. Second, all Tornado Coils were deployed using a wire-push technique; a saline-flush technique was not attempted. Because the tip of a thinner microcatheter is highly flexible, the microcatheter tip may become dislodged if the saline-flush technique is used to deploy the Tornado Coils. Third, all coil embolization procedures were performed when the microcatheters were advanced into small target vessels. We do not recommend coil embolization through a thinner microcatheter in large vessels or at the proximal site because the catheter tip is not stabilized. Conventional microcatheters should be used when microcoil placement is attempted in the proximal portion of a large vessel. Fourth, the Liquid Coil has been discontinued and is no longer available, so currently we only use Tornado Coils. Finally, the trial of coil embolization through a thinner microcatheter should be performed with the personal responsibility of each interventional radiologist.

## Conclusion

Liquid Coils and Tornado Coils can be placed through a microcatheter with a tip of 2F or less without difficulty. The catheter tip may not become dislodged during coil deployment when coil embolization is performed at the distal level. However, we do not recommend coil embolization through a thinner microcatheter in large vessels or at proximal sites because the catheter tip is not stabilized.

## References


1. Okazaki M, Higashihara H, Koganemaru F, Ono H, Fujimitsu R, Yamasaki R, et al. Emergent embolization for control of massive hemorrhage from a splanchnic artery with a new coaxial catheter system. Acta Radiol 1992;33:57–62.
2. Miyayama S, Matsui O, Taki K, Minami T, Ito C, Shinmura R, et al. Combined use of an occlusion balloon catheter and a microcatheter for embolization of the unselectable right inferior phrenic artery supplying hepatocellular carcinoma. Cardiovasc Intervent Radiol 2004;27:677–81.
3. Miyayama S, Matsui O, Yamashiro M, Ryu Y, Kaito K, Ozaki K, et al. Ultraselective transcatheter arterial chemoembolization with a 2-F tip microcatheter for small hepatocellular carcinomas: relationship between local tumor recurrence and visualization of portal vein with iodized oil. J Vasc Interv Radiol 2007;18:365–76.
4. Ha-Kawa SK, Kariya H, Murata T, Tanaka Y. Successful transcatheter embolotherapy with a new platinum microcoil: the Berenstein Liquid coil. Cardiovasc Intervent Radiol 1998;21:297–9.
5. Osuga K, White RI Jr. Micronester: a new pushable fibered microcoil for embolotherapy. Cardiovasc Intervent Radiol 2003;26:554–6.
6. Irie T. New embolization microcoil consisting of firm and flexible segments: preliminary clinical experience. Cardiovasc Intervent Radiol 2006;29:986–90.
7. Tajima T, Yoshimitsu K, Irie H, Nishie A, Hirakawa M, Ishigami K, et al. Microcoil embolization through a downsized coaxial catheter system: an experimental study. Acta Radiol 2009;50:469–73.

Jpn J Radiol (2011) 29:371–377
DOI 10.1007/s11604-011-0568-8

PICTORIAL ESSAY

# Efficacy of cone-beam computed tomography during transcatheter arterial chemoembolization for hepatocellular carcinoma

**Shiro Miyayama · Masashi Yamashiro · Yuki Hattori
Nobuaki Orito · Ken Matsui · Kazunobu Tsuji
Miki Yoshida · Osamu Matsui**

Received: October 12, 2010 / Accepted: January 20, 2011


**Abstract** Cone-beam computed tomography (CBCT) using a flat-panel detector is an alternative method of obtaining cross-sectional images. This technique is now being used during transcatheter arterial chemoembolization (TACE) for inoperable hepatocellular carcinoma (HCC). Several CBCT techniques are performed to detect HCC lesions: CBCT during portography (CBCTAP), CBCT during hepatic arteriography (CBCTHA), CBCT after iodized oil injection (LipCBCT), CBCT during arteriography (CBCTA) of extrahepatic collaterals. Almost all HCC lesions can be detected using these CBCT images. Three-dimensional arteriography using maximum intensity projection from CBCTHA images can identify the tumor-feeding branch. In particular, this technique is useful when the tumor stain cannot be demonstrated on arteriography. In addition, dual-phase CBCTHA can improve the diagnostic accuracy for hypervascular HCCs because corona enhancement can be detected around the tumor. To monitor the embolized area during TACE, selective CBCTHA or LipCBCT at the embolization point is useful. Two sequential CBCT scans without and with contrast material injection is also useful to confirm each embolized area of two vessels. Furthermore, CBCTA can prevent nontarget embolization. Although the image quality of CBCT is low compared to that of conventional CT, CBCT provides useful information that helps perform TACE for HCCs safely and effectively.

**Key words** Cone-beam computed tomography · Hepatocellular carcinoma · Transcatheter arterial chemoembolization

S. Miyayama (✉) · M. Yamashiro · Y. Hattori · N. Orito · K. Matsui · K. Tsuji · M. Yoshida
Department of Diagnostic Radiology, Fukuiken Saiseikai Hospital, 7-1 Funabashi, Wadanaka-cho, Fukui 918-8503, Japan
Tel. +81-776-23-1111; Fax +81-776-28-8519
e-mail: s-miyayama@fukui.saiseikai.or.jp

O. Matsui
Department of Radiology, Kanazawa University Graduate School of Medical Science, Kanazawa, Japan

## Introduction

Transcatheter arterial chemoembolization (TACE) is one of the effective treatments for inoperable hepatocellular carcinoma (HCC). During the TACE procedure, computed tomography (CT)—during arterial portography (CTAP) and during hepatic arteriography (CTHA)—is helpful for identifying hypervascular HCC lesions for treatment.

To perform TACE effectively, superselective catheterization is essential not only through hepatic branches but also through extrahepatic collaterals. However, small tumor-feeding branches may be missed when the catheter is advanced too far into the tumor-feeding branches.[1] In addition, complications may develop when nontumor-feeding extrahepatic branches are inadvertently embolized.[2–5] Intraprocedural monitoring of the embolized area is necessary to improve local control while reducing adverse effects of TACE.[6]

Cone-beam CT (CBCT) technology using a flat-panel detector (FPD) is an alternative method of obtaining cross-sectional images. This technique is currently being combined with TACE for HCC.[7–12] In this article, we describe the efficacy of CBCT during TACE for HCC.

## CBCT technique

An angiographic unit with an FPD can obtain CBCT images. In our CBCT protocol (XperCT; Philips Medical Systems, Best, the Netherlands), 321 projection images with X-ray parameters of 120 kV and 50–325 mA are obtained by 10.4-s acquisition with 207° rotation of a 30 × 38 cm FPD of the angiographic C-arm around the patient. CBCT can be obtained simply by lifting the patients' hands, without other movement. The maximum radiation dose of a single CBCT measured on a CT phantom is 22.3 mGy. Since August 2009, we have used a prototype of the dual-phase CBCT software (Philips Medical Systems). The first phase is scanned during a clockwise rotation and the second phase during a counterclockwise rotation. The minimum interval between the end of the first scan and the start of the second scan is 4 s.

Optimal thick cross-sectional images are obtained for observation of CBCT images on a workstation (Philips Medical Systems). The matrix size is 512 × 512, and the field of view (FOV) is 25 cm. Maximum intensity projection (MIP) images from CBCT can also be used to observe the vascular anatomy.

## Detection of HCC by CBCT

Several CBCT techniques are performed during the TACE procedure: during arterial portography (CBCTAP), during hepatic arteriography (CBCTHA), and after iodized oil (Lipiodol; Andre Guerbet, Aulnay-sous-Bois, France) injection (LipCBCT). All three techniques correspond to CTAP, CTHA, and Lipiodol-CT obtained by a conventional CT scanner. During CBCTAP, 40 ml of contrast material [370 mg I iopamidol (Iopamiron 370); Bayer, Osaka, Japan] is injected at a rate of 3 ml/s through a 4F catheter placed into the superior mesenteric artery after administration of 2.5 μg of prostaglandin $E_1$ ($PGE_1$) (Liple; Tanabe Mitsubishi, Osaka, Japan). When the replaced hepatic branches or arterial flow toward the liver from the superior mesenteric artery is demonstrated, the catheter tip is deeply advanced avoiding these branches. Scanning begins 25 s after the start of the contrast material injection. CBCTHA is performed during the common or proper hepatic, right or left hepatic, or selective arteriography of the liver. When CBCTHA is performed at the common or proper hepatic artery, 25–40 ml of half-diluted contrast material is injected at a rate of 1.5–2.0 ml/s through a 4F catheter. When CBCTHA is performed at a more distal level of the right or left hepatic artery (selective CBCTHA), 5–10 ml of half-diluted contrast material is slowly injected manually through a microcatheter. Scanning starts 7 s after the beginning of the contrast material injection. LipCBCT is also performed after injection of a mixture of 1–3 ml of iodized oil and anticancer drugs. This technique is mainly performed when blood supply to the tumor from the selected branch is highly suspected or when iodized oil accumulation in the tumor is unclear during TACE despite tumor feeding on selective CBCTHA images. In addition, this technique is performed when the selected branch is minute, and contrast material easily overflows despite careful hand injection. CBCT during arteriography (CBCTA) of extrahepatic collaterals is also performed to confirm an extrahepatic blood supply to an HCC using 5–10 ml of half-diluted contrast material.

In a previous report, 89% of HCC nodules (mean diameter ± standard deviation, 1.9 ± 1.1 cm) could be detected by CBCTAP compared to conventional CTAP.[9] In addition, all small HCCs (mean diameter 1.3 ± 0.3 cm) that could not be detected on arteriography could be depicted by combined with CBCTAP, CBCTHA, and LipCBCT (Figs. 1–11).[10] Among these images, LipCBCT is the most sensitive for detecting small HCC nodules because of the high contrast of iodized oil (Fig. 2).[10]

## Detection of corona enhancement around HCC

Corona enhancement represents venous drainage through hypervascular HCC nodules.[13,14] It is one of the most reliable findings for distinguishing between HCCs and arterioportal shunts.[15] In a previous report, corona enhancement was detected in 89% of HCC lesions. It had a mean diameter of 1.8 ± 0.9 cm on second-phase CBCTHA images obtained 30 s after the end of the first scan (Figs. 3, 4; see also Fig. 11, below), although it could not be detected around small tumors.[12] In contrast, corona enhancement is not seen around hypervascular pseudolesions, such as arterioportal shunts (Fig. 4).[12,15] This technique can improve the diagnostic accuracy of hypervascular HCC nodules by CBCTHA. In addition, the area of corona enhancement should be included to the safety margin of the treatment because HCC cells spread mainly via the drainage route. Therefore, depiction of corona enhancement on CBCTHA is meaningful when determining the adequacy of the embolized area during TACE.

## Identification of tumor-feeding branch

Slab-MIP images from CBCTHA can identify not only the tumor stain but also the tumor-feeding branch.[11] These images are particularly useful when a tumor stain is unclear on arteriography. Observation of slab-MIP images at the optional thickness and direction using a

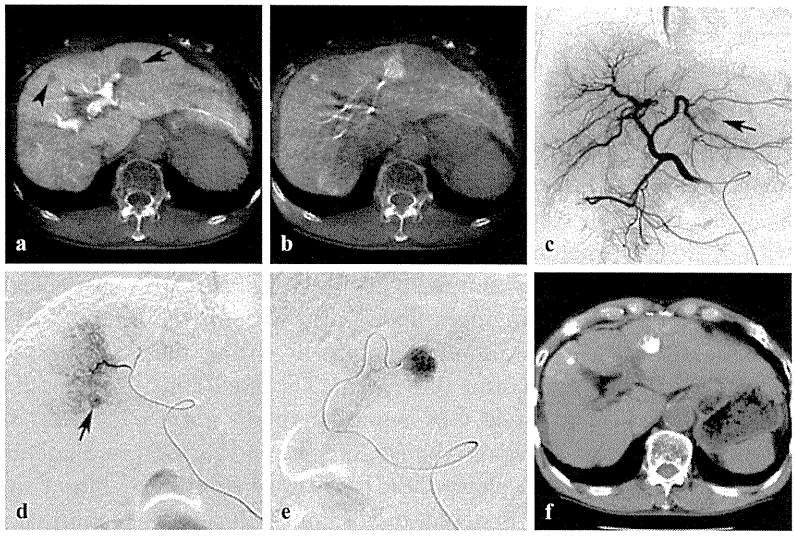


**Fig. 1.** **a** Cone-beam computed tomography during arterial portography (CBCTAP) shows hypoattenuating nodules in segments III (*arrow*) and IV (*arrowhead*). **b** On CBCT during hepatic arteriography (CBCTHA), both lesions show enhancement. Artifacts from the contrast material in the vessels are also seen. **c** Common hepatic arteriography shows a tumor stain in the left lobe of the liver (*arrow*). The tumor in segment IV is not demonstrated. **d** First, one branch of the anterior inferior subsegmental artery of the right hepatic artery was selected. Selective arteriography shows a tumor stain (*arrow*). Therefore, transcatheter arterial chemoembolization (TACE) was performed. **e** Subsequently, the tumor-feeding branch of the large tumor was selected, and TACE was performed. **f** Unenhanced CT performed 1 week after TACE shows dense iodized oil accumulation in both tumors

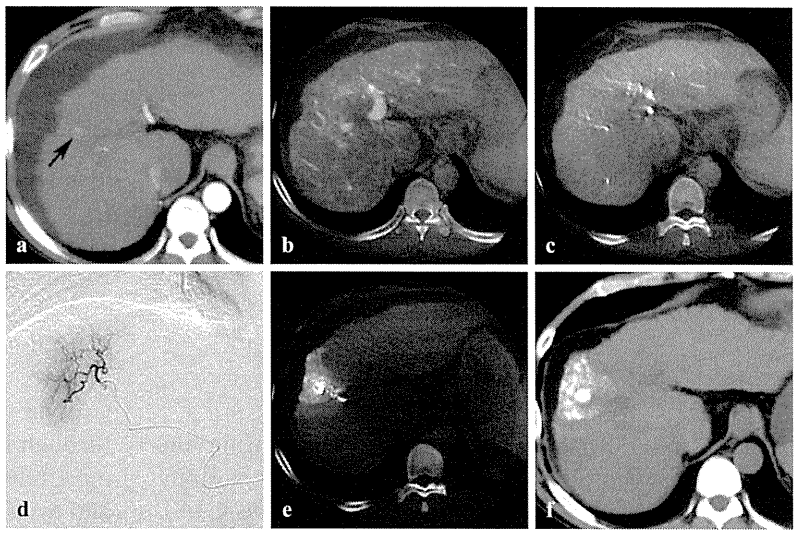


**Fig. 2.** **a** Arterial phase CT shows a small tumor in segment V (*arrow*). **b** On CBCTAP, the tumor is unclear. **c** It is also unclear on CBCTHA. **d** Based on the anatomical tumor location, a branch of the anterior inferior subsegmental artery of the right hepatic artery, suspected of being a tumor-feeding branch, was selected; and a mixture of iodized oil and anticancer drug was injected. **e** On CBCT after iodized oil injection (LipCBCT), the iodized oil was densely accumulated in the tumor with an adequate safety margin around the tumor. TACE was then completed. **f** Unenhanced CT performed 1 week after TACE shows dense iodized oil accumulation in the tumor

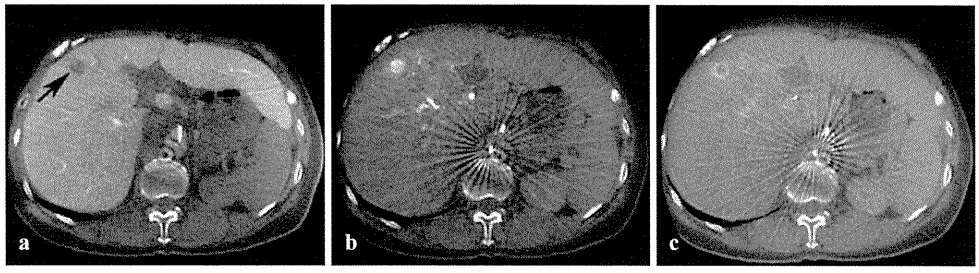


**Fig. 3.** **a** CBCTAP shows a small hypoattenuating nodule in segment V (*arrow*). **b** CBCTHA via the replaced right hepatic artery shows nodular enhancement. The radial artifacts from the catheter are also seen. **c** On second-phase CBCTHA, corona enhancement is clearly seen around the tumor


**Fig. 4.** **a** Coronal view of CBCTAP image shows a round, hypoattenuating area (*arrow*) and an amorphous hypoattenuating area in segment III (*arrowhead*). **b** On CBCTHA, both lesions show enhancement. **c** On second-phase CBCTHA, the round lesion shows corona enhancement, so the lesion is diagnosed as hepatocellular carcinoma (HCC). In contrast, the amorphous lesion shows prolonged enhancement without corona enhancement, and the lesion was diagnosed as an arterioportal shunt

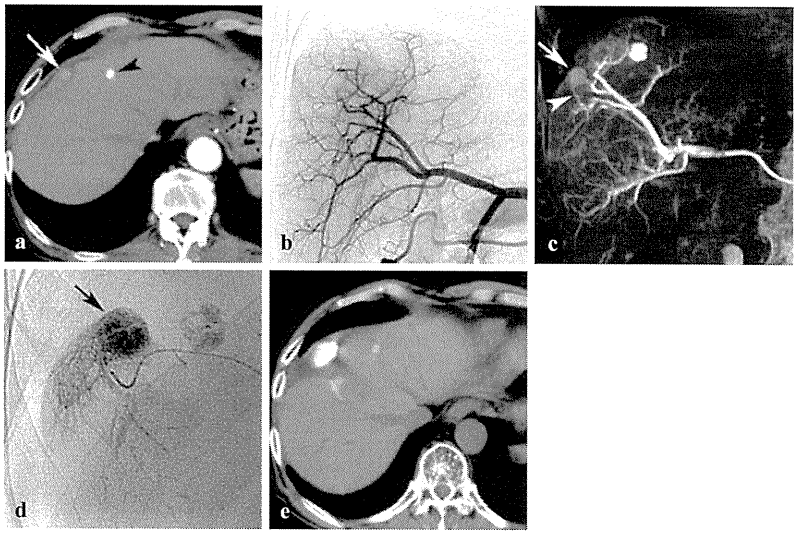


**Fig. 5.** **a** Arterial phase CT shows a small tumor in segment V (*arrow*). Another tumor that had previously been treated by TACE is also seen (*arrowhead*). **b** Common hepatic arteriography does not show any obvious tumor staining. **c** Oblique coronal maximum intensity projection (MIP) image from CBCTHA shows a tumor stain (*arrow*) fed by a small branch of the anterior inferior subsegmental artery of the right hepatic artery (*arrowhead*). **d** The branch was selected, and TACE was performed. The *arrow* indicates the tumor. **e** Unenhanced CT performed 1 week after TACE shows dense iodized oil accumulation in a limited area including the tumor

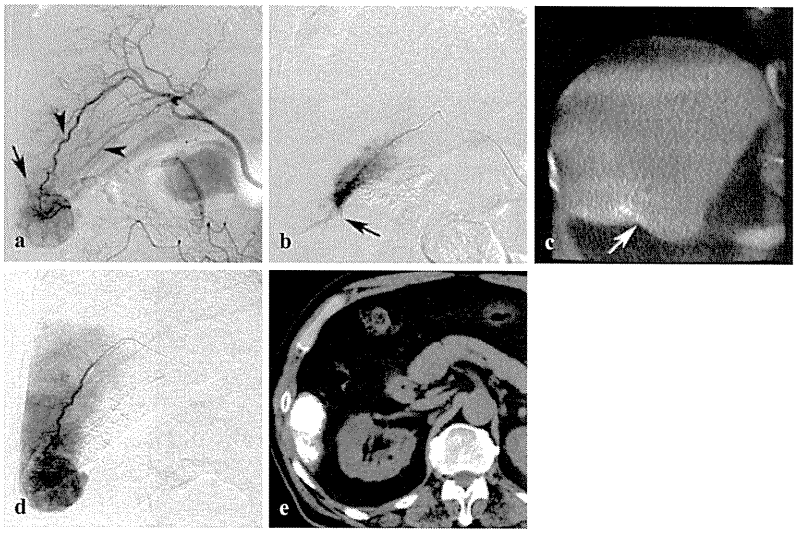


**Fig. 6.** **a** Arteriogram of the right hepatic artery shows a large tumor and an intrahepatic metastasis (*arrow*). Two branches were suspected of feeding the tumor (*arrowheads*). **b** First, a small branch of the posterior inferior subsegmental artery of the right hepatic artery was selected. Arteriography of this vessel shows a small tumor-feeding branch (*arrow*). **c** Sagittal view of CBCTHA image at this branch shows a partial tumor stain (*arrow*). Therefore, TACE was performed through this branch. **d** Second, the main feeding branch of the anterior inferior subsegmental artery of the right hepatic artery was selected, and TACE was performed. **e** Unenhanced CT performed 1 week after TACE shows dense iodized oil accumulation in the tumor and surrounding liver parenchyma

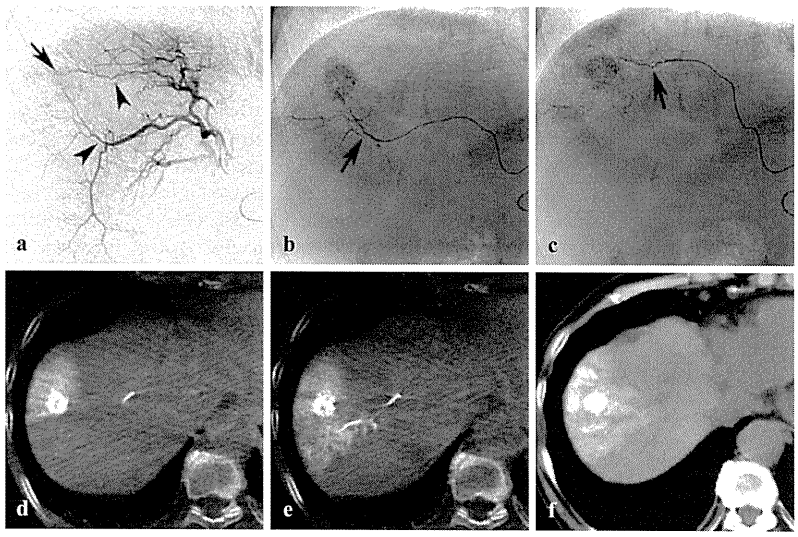


**Fig. 7.** **a** Arteriography of the anterior segmental artery of the right hepatic artery shows a faint tumor stain (*arrow*). Two branches were suspected of feeding the tumor (*arrowheads*). **b** First, one branch of the anterior inferior subsegmental artery was selected, and TACE was performed. The *arrow* shows the catheter tip. **c** Thereafter, the microcatheter was advanced into one branch of the anterior superior subsegmental artery and two-sequence CBCT was performed. The *arrow* shows the catheter tip. **d** The first scan obtained without contrast material injection shows that iodized oil does not distribute into the dorsal portion near the tumor. **e** The second scan obtained during injection of diluted contrast material through the microcatheter shows that contrast material distributes into the dorsal portion near the tumor. TACE was also performed at that point. **f** CT performed 1 week after TACE shows that the entire tumor is embolized with an adequate safety margin

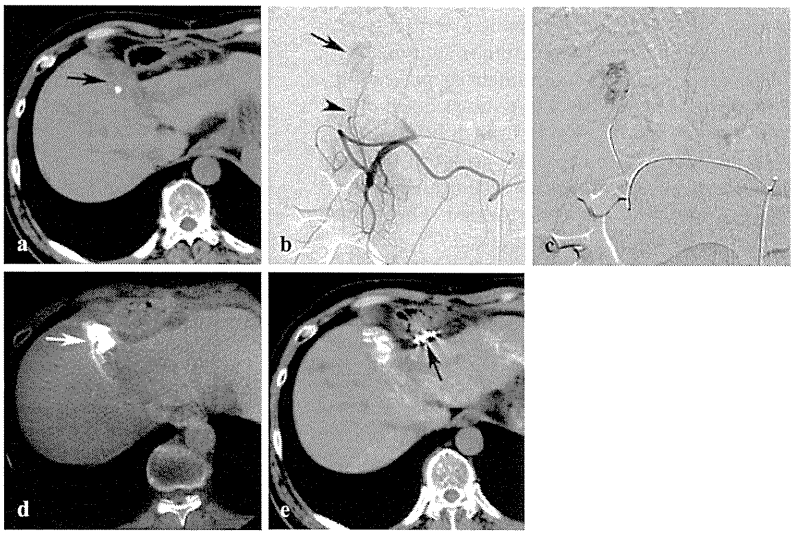


**Fig. 8.** **a** Unenhanced CT shows a recurrent tumor near the iodized oil accumulation in the previously treated tumor (*arrow*). **b** Arteriography of the gastroduodenal artery shows a tumor stain (*arrow*) supplied by the duodenal branch (*arrowhead*). **c** The tumor-feeding branch was selected. **d** CBCT at the embolization point shows a tumor stain (*arrow*). **e** Unenhanced CT performed 1 week after TACE shows iodized oil accumulation in the tumor. The *arrow* shows metallic coils placed in the right gastric artery to embolize another tumor (not shown)

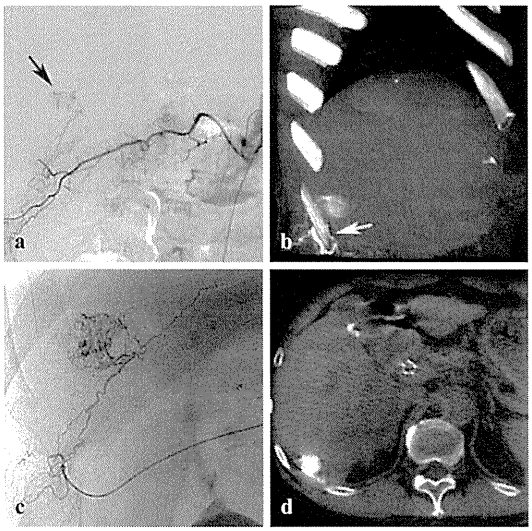


**Fig. 9.** **a** Arteriography of the right subcostal artery shows a tumor stain (*arrow*). **b** Sagittal view of an MIP image from CBCTA of the right subcostal artery shows a tumor-feeding branch with a sharp upward turn (*arrow*). **c** The microcatheter was advanced into the tumor-feeding branch, and TACE was performed. **d** CBCTHA at the embolization point does not show any enhancement of muscle tissues. Subsequently, TACE was performed

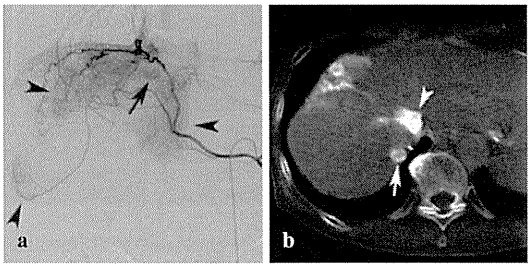


**Fig. 10.** **a** Arteriography of the right inferior phrenic artery shows a nodular stain (*arrow*) and amorphous stains (*arrowheads*). **b** CBCT during arteriography (CBCTA) at the right inferior phrenic artery shows a tumor in segment VII (*arrow*) and segmental enhancement of the caudate lobe (*arrowhead*)

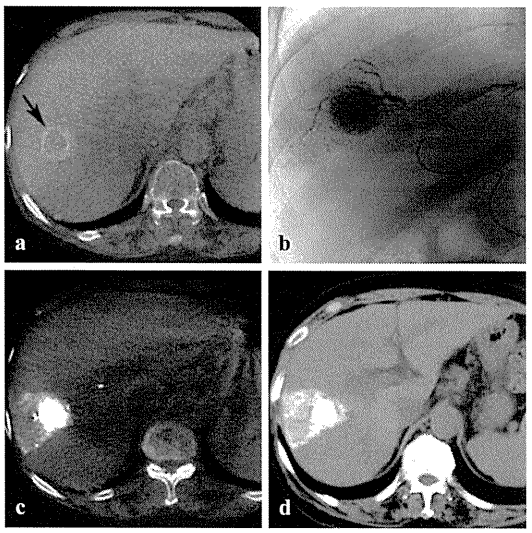


**Fig. 11.** **a** Second-phase CBCTHA shows a tumor with thick corona enhancement in segment V (*arrow*). **b** One branch of the anterior inferior subsegmental artery of the right hepatic artery was embolized. **c** LipCBCT shows dense iodized oil accumulation in the tumor with a safety margin. **d** Unenhanced CT performed 1 week after TACE also shows that the tumor is completely embolized

workstation can easily recognize the branching pattern of the feeder, and helpful information is provided for performing superselective catheterization (Fig. 5).

## Confirmation of embolized area

Selective CBCTHA or LipCBCT at the embolization point can indicate the embolized area (Fig. 2).[10] Observation at the optimal direction of CBCT images is useful to confirm that the target tumor is entirely embedded in the embolized area with an adequate safety margin.

The HCC nodules frequently have multiple feeding branches. For large tumors, the main feeding branch should be embolized last because dense retention of iodized oil and contrast material in the tumor and liver parenchyma just after TACE makes it difficult to confirm the residual tumor.[1] CBCT can provide useful information for determining the order of embolization for each feeder (Fig. 6). In contrast, for small tumors, the order of embolization of each feeder is not strict because artifacts from iodized oil and contrast material do not reduce the image quality as much (Fig. 7).

The two-sequence CBCT technique without and with contrast material injection is also useful for confirming each embolized area of two vessels during TACE when the tumor is supplied by two feeding branches (Fig. 7). After embolization of one feeding branch, the catheter is advanced into the other feeding branch. The first scan is then obtained without contrast material injection, followed by the second scan after contrast material is injected through the catheter. The first CBCT images depict the iodized oil distribution in the vascular territory of the feeding branch that was embolized immediately before the scan, and the second set of CBCT images indicate the vascular territory of the other feeding branch just selected by the catheter. This technique may improve the technical success rates of ultraselective TACE and may reduce the effort and procedural duration. If the scan becomes faster, it will become possible to obtain these two sequential images during a single breath-hold.

### Prevention of nontarget embolization

TACE through extrahepatic vessels may cause severe complications when a nontarget branch is embolized.[2–5] CBCTA through extrahepatic collateral vessels is useful for avoiding nontarget embolization (Figs. 8, 9). When CBCTA shows enhancement of the nontumor tissues as well as tumor staining, the catheter should be distally advanced into the tumor-feeding branch to prevent unnecessary embolization of vessels that do not supply the tumor (Fig. 9). In addition, CBCTA is useful for distinguishing between tumor staining and nontumor staining, which is seen most frequently with arteriography of the inferior phrenic artery (Fig. 10).

### Recognition of endpoints of TACE

The goal of TACE for HCC is that the target tumor is embolized with an adequate safety margin (Fig. 11). CBCT can confirm that the endpoint of TACE has been reached. Local control effects of TACE may be improved and adverse effects reduced when intraprocedural monitoring of embolized areas is performed by CBCT.

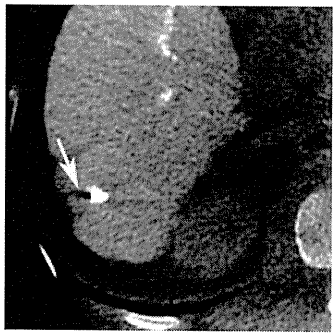

**Fig. 12.** On CBCTAP, note the artifacts from densely concentrated iodized oil (*arrow*)

In a previous report, 82% of small HCCs that could not be detected by angiography could be embolized with an adequate safety margin at least 5 mm wide using two to six (mean 3.8 ± 1.1) CBCT procedures.[10]

### Limitations of CBCT

An advantage of CBCT technology is that it can reduce the irradiation dose compared to that used during conventional CT.[7] There are also some disadvantages. CBCT images have several noises, in particular at the central portion of the FOV. In addition, CBCT images are low contrast, and motion artifacts mainly caused by inadequate breath-holding deteriorates the image quality. Artifacts from the catheter, contrast material in the vessels, or densely accumulated iodized oil are also seen (Figs. 1, 3, 12).[9] An advanced algorithm and a faster scanning protocol to reduce these image artifacts may be needed to improve the image quality. The FOV of CBCT is also too small to observe the entire liver.[9] HCC nodules located in the lateral segment of the liver are not included in the FOV of CBCT in large patients when the right lobe of the liver is entirely included in the FOV.

## Conclusion

Cone-beam computed tomography using an FPD is an alternative method of obtaining cross-sectional images. The image quality of CBCT is low compared to that of conventional CT, but CBCT provides useful information about performing TACE for HCC safely and effectively with little effort.

## References

1. Miyayama S, Matsui O, Yamashiro M, Ryu Y, Kaito K, Ozaki K, et al. Ultraselective transcatheter arterial chemoembolization with a 2-F tip microcatheter for small hepatocellular carcinomas: relationship between local tumor recurrence

and visualization of the portal vein with iodized oil. J Vasc Interv Radiol 2007;18:365–76.
2. Takayasu K, Moriyama N, Muramatsu Y, Shima Y, Ushio K, Yamada T, et al. Gallbladder infarction after hepatic artery embolization. AJR Am J Roentgenol 1985;144:135–8.
3. Arora R, Soulen MC, Haskal ZJ. Cutaneous complications of hepatic chemoembolization via extrahepatic collaterals. J Vasc Interv Radiol 1999;10:1351–6.
4. Kim HC, Chung JW, Lee W, Jae HJ, Park JH. Recognizing extrahepatic collateral vessels that supply hepatocellular carcinoma to avoid complications of transcatheter arterial chemoembolization. Radiographics 2005;25:S25–39.
5. Miyayama S, Matsui O, Taki K, Minami T, Ryu Y, Ito C, et al. Extrahepatic blood supply to hepatocellular carcinoma: angiographic demonstration and transcatheter arterial chemoembolization. Cardiovasc Intervent Radiol 2006;29:39–48.
6. Takayasu K, Muramatsu Y, Maeda T, Iwata R, Furukawa H, Muramatsu Y, et al. Targeted transarterial oily chemoembolization for small foci of hepatocellular carcinoma using a unified helical CT and angiography system: analysis of factors affecting local recurrence and survival rates. AJR Am J Roentogenol 2001;176:681–8.
7. Hirota S, Nakao N, Yamamoto S, Kobayashi K, Maeda H, Ishikawa R, et al. Cone-beam CT with flat-panel-detector digital angiography system: early experience in abdominal interventional procedures. Cardiovasc Intervent Radiol 2006;29:1034–8.
8. Kakeda S, Korogi Y, Ohnari N, Moriya J, Oda N, Nishino K, et al. Usefulness of cone-beam CT with flat panel detectors in conjunction with catheter angiography for transcatheter arterial embolization. J Vasc Interv Radiol 2007;18:1508–16.
9. Miyayama S, Matsui O, Yamashiro M, Ryu Y, Takata H, Takeda T, et al. Detection of hepatocellular carcinoma by CT during arterial portography using a cone-beam CT technology: comparison with conventional CTAP. Abdom Imaging 2009;34:502–6.
10. Miyayama S, Yamashiro M, Okuda M, Yoshie Y, Sugimori N, Igarashi S, et al. Usefulness of cone-beam computed tomography during ultraselective transcatheter arterial chemoembolization for small hepatocellular carcinomas that cannot be demonstrated on angiography. Cardiovasc Intervent Radiol 2009;32:255–64.
11. Tognolini A, Louie JD, Hwang GL, Hofmann LV, Sze DY, Kothary N. Utility of C-arm CT in patients with hepatocellular carcinoma undergoing transhepatic arterial chemoembolization. J Vasc Interv Radiol 2010;21:339–47.
12. Miyayama S, Yamashiro M, Okuda M, Yoshie Y, Nakashima Y, Ikeno H, et al. Detection of corona enhancement of hypervascular hepatocellular carcinoma by C-arm dual-phase cone-beam CT during hepatic arteriography. Cardiovasc Intervent Radiol 2011;34:81–6.
13. Ueda K, Matsui O, Kawamori Y, Nakanuma Y, Kadoya M, Yoshikawa J, et al. Hypervascular hepatocellular carcinoma: evaluation of hemodynamics with dynamic CT during hepatic arteriography. Radiology 1998;206:161–6.
14. Kitao A, Zen Y, Matsui O, Gabata T, Nakanuma Y. Hepatocarcinogenesis: multistep changes of drainage vessels at CT during arterial portography and hepatic arteriography—radiologic-pathologic correlation. Radiology 2009;252:605–14.
15. Ueda K, Matsui O, Kawamori Y, Kadoya M, Yoshikawa J, Gabata T, et al. Differentiation of hypervascular hepatic pseudolesions from hepatocellular carcinoma: value of single-level dynamic CT during hepatic arteriography. J Comput Assist Tomogr 1998;22:703–8.

Cardiovasc Intervent Radiol
DOI 10.1007/s00270-011-0328-2

CLINICAL INVESTIGATION

# Origins of Feeding Arteries of Hepatocellular Carcinoma Located Near the Umbilical Fissure of the Left Hepatic Lobe: Angiographic Evaluation

**Shiro Miyayama · Masashi Yamashiro · Yoshihiro Shibata · Masahiro Hashimoto · Miki Yoshida · Kazunobu Tsuji · Fumihito Toshima · Osamu Matsui**

Received: 3 October 2011 / Accepted: 23 November 2011


**Abstract**
*Purpose* To analyze the origins of the feeding arteries of hepatocellular carcinomas (HCCs) near the umbilical fissure of the left hepatic lobe.
*Methods* Twenty-eight HCCs with a mean ± SD tumor diameter of 3.4 ± 1.0 cm (range 1–4.4 cm) in contact with the right or left side of the umbilical fissure were treated by superselective transcatheter arterial chemoembolization (TACE). The origins of the tumor-feeding arteries were analyzed with arteriograms and computed tomography or cone-beam computed tomography images obtained during and 1 week after TACE.
*Results* Twenty-one HCC lesions were located in segment 3 and seven were located in segment 4. Of 21 tumors in segment 3, 13 (61.9%) were supplied by the lateral inferior subsegmental artery (A3), three (14.3%) by the medial subsegmental artery (A4), three (14.3%) by both A4 and A3, one (4.8%) by a branch arising from the left lateral hepatic artery, and one (4.8%) by a branch of the right gastric artery. In particular, all tumor-feeding branches arising from A4 were the first branch of A4. Of seven tumors in segment 4, four (57.1%) were supplied by A4 and three (42.9%) by A3. In particular, all tumor-feeding branches arising from A3 were the first branch of A3.
*Conclusion* This study demonstrates crossover blood supply to HCC lesions located near the umbilical fissure, in addition to direct feeding from a separate branch. In particular, the first branch of the opposite subsegmental artery may feed tumors when crossover blood supply is present.

**Keywords** Feeding artery · Hepatocellular carcinoma · Transcatheter arterial chemoembolization · Umbilical fissure

## Introduction

Transcatheter arterial chemoembolization (TACE) is one of the most effective treatments for inoperable hepatocellular carcinoma (HCC), and it is performed worldwide [1–4]. Superselective catheterization into the tumor-feeding branches with a microcatheter is essential to enhance the therapeutic effects and to reduce the adverse effects of TACE [2–4].

The left hepatic lobe is divided into the medial and lateral segments by the umbilical fissure, which consists of the parietal surface of the falciform ligament attachment and the visceral surface of the fissure for the ligamentum venosum and ligamentum teres [5–7]. However, it is reported that small branches of the bile duct and vessels infrequently cross the umbilical fissure [7–10]. Therefore, it is important to recognize the arterial blood supply to HCC lesions near the umbilical fissure to perform effective TACE.

The purpose of this study was to evaluate the origins of the feeding arteries of HCCs located near the umbilical fissure.

## Materials and Methods

We retrospectively analyzed the origins of the feeding arteries of HCCs near the umbilical fissure. Institutional

S. Miyayama (✉) · M. Yamashiro · Y. Shibata · M. Hashimoto · M. Yoshida · K. Tsuji · F. Toshima
Department of Diagnostic Radiology, Fukuiken Saiseikai Hospital, 7-1, Funabashi, Wadanaka-cho, Fukui 918-8503, Japan
e-mail: s-miyayama@fukui.saiseikai.or.jp

O. Matsui
Department of Radiology, Kanazawa University Graduate School of Medical Science, 13-1, Takara-machi, Kanazawa 920-8641, Japan

Published online: 16 December 2011

review board approval is not required at our institution for this type of study. Written informed consent was obtained from each patient before the TACE procedure.

### Patients

We selected newly developed HCCs <5 cm in diameter in contact with the right or left surface of the umbilical fissure (Fig. 1), not extending over both sides of the umbilical fissure, and treated by superselective TACE. Although we are well aware that the umbilical fissure is present between segments 2 and 4, tumors located in segment 2 and in the cranial part of segment 4 were excluded from the present study because the falciform ligament was not always outlined clearly on computed tomography (CT) at the cranial part of the left hepatic lobe. We also excluded HCCs that were locally recurrent tumors after previous treatment including TACE, HCCs that were newly developed but for which TACE to segments 3 and 4 had previously been performed, and HCCs that were initially treated by TACE at the left hepatic artery level in a nonselective fashion. Between October 2001 and July 2011, a total of 28 HCC lesions in 28 patients met the above criteria. There were 18 men and 10 women in the study with a mean ± SD patient age of 71.3 ± 9.1 years (range 56–89 years). All patients had chronic hepatitis or liver cirrhosis. This was related to hepatitis C in 22 patients and hepatitis B in two patients. The etiology was unknown in four patients. Fifteen patients had no history of any treatment for HCC. Thirteen patients had previously undergone 1–8 TACE sessions (3.2 ± 2.1) for HCCs except for segments 3 and 4.

All patients had a single HCC lesion located near the umbilical fissure with a mean tumor diameter of 3.4 ± 1.0 cm (range 1–4.4 cm). Fourteen patients also had other viable HCC lesions besides the tumor near the umbilical fissure. The diagnosis of HCC was made by imaging findings: nodular staining and washout on dynamic CT and/or dynamic magnetic resonance imaging; nodular staining on arteriography and/or CT during hepatic arteriography; and nodular perfusion defect on CT during arterial portography, in addition to hyperintensity on T2-weighted and diffusion-weighted magnetic resonance imaging.

### TACE Procedure

TACE was performed at the more distal level to the subsegmental artery through a 1.8–2.4F tip microcatheter (Carnelian Pixie ER; Tokai Medical Products, Kasugai, Japan, Progreat α, Σ; Terumo, Tokyo, Japan; and Microferret-18; Cook, Bloomington, IN) with 2–4 ml of iodized oil (Lipiodol; Andre Guerbet, Aulnaysous-Bois, France) and anticancer drugs (10–20 mg of epirubicin [Farmorbicin; Pfizer, Tokyo, Japan] and 2–4 mg of mitomycin C [Mitomycin; Kyowa Hakko Kirin, Tokyo, Japan]), followed by approximately 0.2–0.5-mm gelatin sponge particles (Gelfoam; Upjohn, Kalamazoo, MI; or Gelpart; Nippon Kayaku, Tokyo, Japan). Selective CT or cone-beam CT (CBCT) examination at the TACE point was also performed if necessary. Unenhanced CT was routinely obtained 1 week after TACE to check for the distribution of the iodized oil injected during TACE.

### Assessment

The findings of arteriograms, CT, or CBCT obtained during TACE and CT obtained 1 week after TACE were analyzed to confirm the origins of the feeding arteries of HCCs located near the umbilical fissure. The embolized artery was confirmed as the tumor-feeding artery when selective arteriogram, CT, and/or CBCT demonstrated tumor staining and iodized oil accumulation in the tumor was observed on CT obtained 1 week after TACE.

## Results

Twenty-one HCC lesions (75%) were located at the left side of the umbilical fissure (segment 3) (Figs. 2, 3, 4, 5),

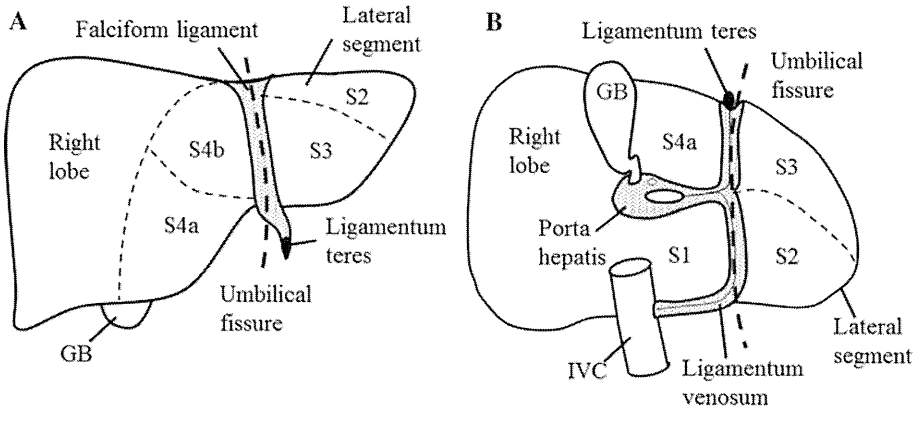


**Fig. 1** Schematic presentation of the umbilical fissure. **A** Frontal view. **B** Caudal view. *GB* gallbladder, *S1* segment 1, *S4* segment 4, *IVC* inferior vena cava. The umbilical fissure is identified as a fat plane between S4 and the lateral segment on CT

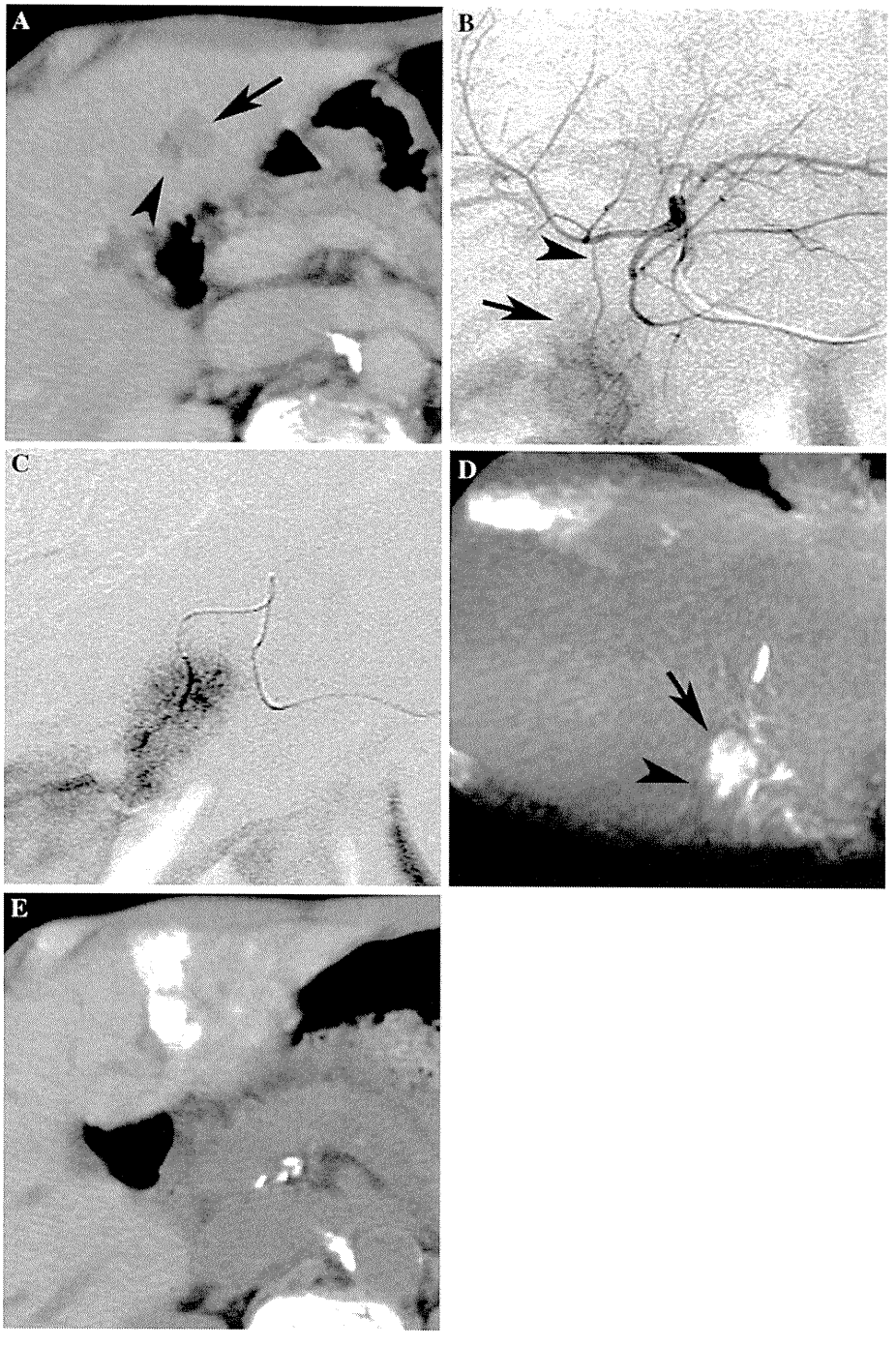


**Fig. 2** HCC located at the left side of the umbilical fissure in an 80-year-old man. **A** CT revealed a tumor (*arrow*) at the left side of the umbilical fissure (*arrowhead*). **B** Left hepatic arteriogram revealed tumor staining (*arrow*) supplied by the first branch derived from the medial subsegmental artery (A4) (*arrowhead*). **C** Selective arteriogram of the branch revealed tumor staining. TACE was performed at this point. **D** Oblique coronal view of CBCT obtained immediately after TACE of the branch revealed iodized oil accumulation in a tumor (*arrow*) located at the left side of the umbilical fissure (*arrowhead*). Another tumor that was simultaneously embolized was observed in the right hepatic lobe. **E** CT obtained 1 week after TACE revealed dense iodized oil accumulation in a limited area at the left side of the umbilical fissure including the tumor

and seven (25%) were located at the right side of the umbilical fissure (segment 4) (Fig. 6).

Of 21 HCC lesions in segment 3, 13 tumors (61.9%) were supplied by the lateral inferior subsegmental artery (A3), three (14.3%) were supplied by the medial subsegmental artery (A4) (Fig. 2), three (14.3%) were supplied by both A4 and A3 (Fig. 3), one (4.8%) was supplied by a branch directly arising from the left lateral hepatic artery (Fig. 4), and one (4.8%) was supplied by a branch arising from the right gastric artery (Fig. 5). In particular, all tumor-feeding branches arising from A4 were the first branch of A4 (Figs. 2, 3).

Of seven HCC lesions in segment 4, four tumors (57.1%) were supplied by A4 and three (42.9%) were supplied by A3 (Fig. 6). In particular, all tumor-feeding branches arising from A3 were the first branch of A3 (Fig. 6).

There were no anastomoses between any tumor-feeding branches arising from the opposite subsegmental artery and the arterial branches of the tumor-bearing subsegment.

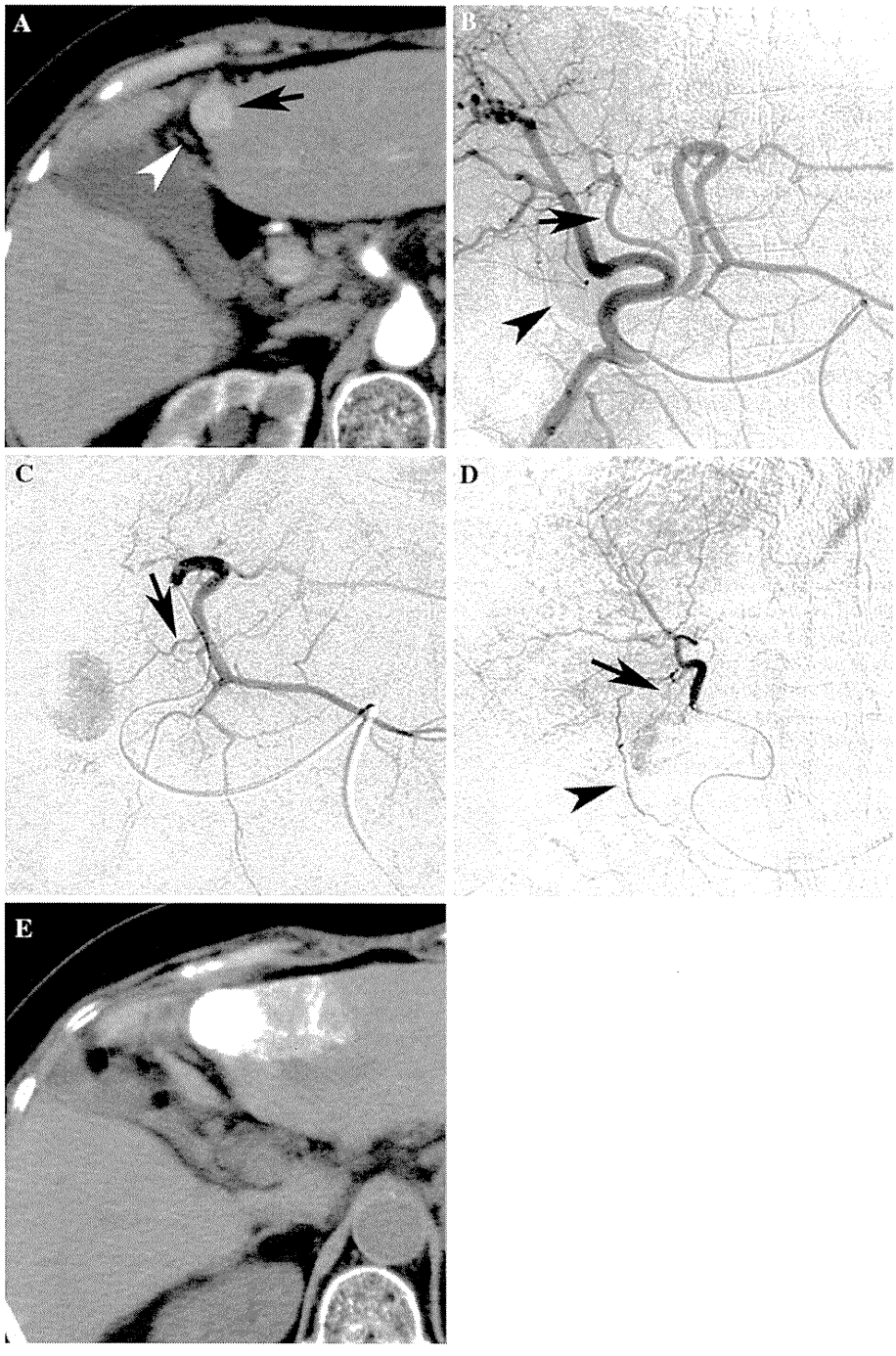


**Fig. 3** HCC located at the left side of the umbilical fissure in a 70-year-old woman. **A** CT revealed a tumor (*arrow*) at the left side of the umbilical fissure (*arrowhead*). **B** Common hepatic arteriogram revealed that A4 arose as the middle hepatic artery (*arrow*). The *arrowhead* indicates tumor staining. **C** Lateral left hepatic arteriogram revealed that the tumor was mainly supplied by the first branch of the lateral inferior subsegmental artery (A3) (*arrow*). **D** Middle hepatic arteriogram also revealed staining at the right side of the tumor supplied by the first branch of A4. The falciform artery was also seen (*arrowhead*). **E** CT obtained 1 week after TACE revealed dense iodized oil accumulation in the tumor

## Discussion

Liver segments, as defined by Couinaud [5], are generally used to describe segmental anatomy. The umbilical fissure, which is the left intersegmental plane, anatomically divides the left hepatic lobe into the medial and lateral segments [5–8]. Therefore, the right side of the umbilical fissure is included in segment 4 and the left side is included in segments 2 and 3.

In a cadaver study by Gupta et al. [7], small branches of the medial segmental duct and blood vessels crossed to the left of the umbilical fissure in 4.7% cases and the lateral segmental duct and blood vessels crossed to the right of the umbilical fissure in 2.4%. Renz et al. [9] reported that biliary radicles originating from segment 4 were identified as crossing the umbilical fissure in 30% of cases. In the present study, the branch of A4 partially or completely supplied 28.6% of HCC lesions in segment 3 near the

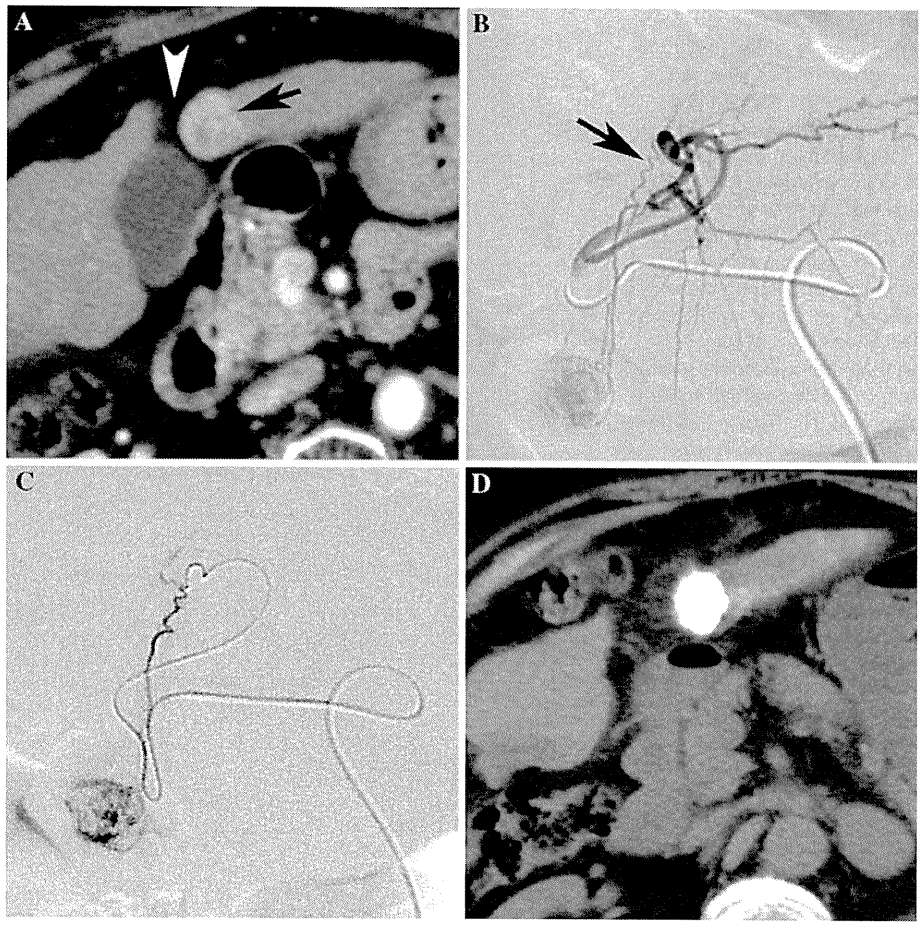


**Fig. 4** HCC located at the left side of the umbilical fissure in a 71-year-old woman. **A** CT revealed a tumor (*arrow*) at the left side of the umbilical fissure (*arrowhead*). **B** Lateral left hepatic arteriogram revealed that the tumor was supplied by a branch directly arising from the lateral segmental artery before the bifurcation of A2 and A3 (*arrow*). **C** Selective arteriogram of the branch revealed tumor staining. **D** CT obtained 1 week after TACE revealed dense iodized oil accumulation in the tumor

umbilical fissure, while the branch of A3 completely supplied 42.9% of HCC lesions in segment 4 near the umbilical fissure. The incidences of crossover blood supply in our results were higher than those of the cadaver or surgical studies. This suggests that small tumor-feeding branches crossing the umbilical fissure become apparent in HCC lesions because the tumors are hypervascular and the feeding branches are usually hypertrophied. In a study by Chen et al. [11] that used carbon dioxide ($CO_2$)-enhanced ultrasonography during hepatic arteriography, crossover blood supply between the medial and left lateral segments was seen in 50% (7 of 14) of cases. However, $CO_2$ may pass through tiny arterioportal communications that cannot be demonstrated on arteriograms using iodinated contrast medium because of its extremely low viscosity [12]. Therefore, it may be impossible to determine whether $CO_2$ is distributed into the opposite liver parenchyma via the artery or portal vein. In addition, intersegmental arterial communications between the medial and left lateral segments are extrahepatically located in the umbilical plate [10]. If the catheter is not deeply advanced into the segmental artery, $CO_2$ may also pass through these intersegmental arterial communications and flow into the opposite liver parenchyma.

In the present study, all tumor-feeding branches arising from the opposite subsegmental artery were the first branch of each subsegmental artery without anastomosis. Cho et al. [10] also reported that the left lateral hepatic artery forked off into branches that crossed the umbilical portion and nourished the liver parenchyma of segment 4 without communicating with the middle hepatic artery in 25% (3 of 12) of cases. Our study suggests that crossover arterial supply between segments 3 and 4 without anastomosis is not clinically rare, not only from segment 3 to segment 4, but also from segment 4 to segment 3.

Additionally, two HCC lesions in segment 3 near the umbilical fissure were supplied by a separate feeding branch arising from the left lateral hepatic artery or right gastric artery. To our knowledge, there are no reports demonstrating this peculiar vascular anatomy supplying a small part of segment 3 near the umbilical fissure.

There is a significant limitation to the present study. We only evaluated crossover blood supply between segments 3 and 4 in patients with HCC near the umbilical fissure. The

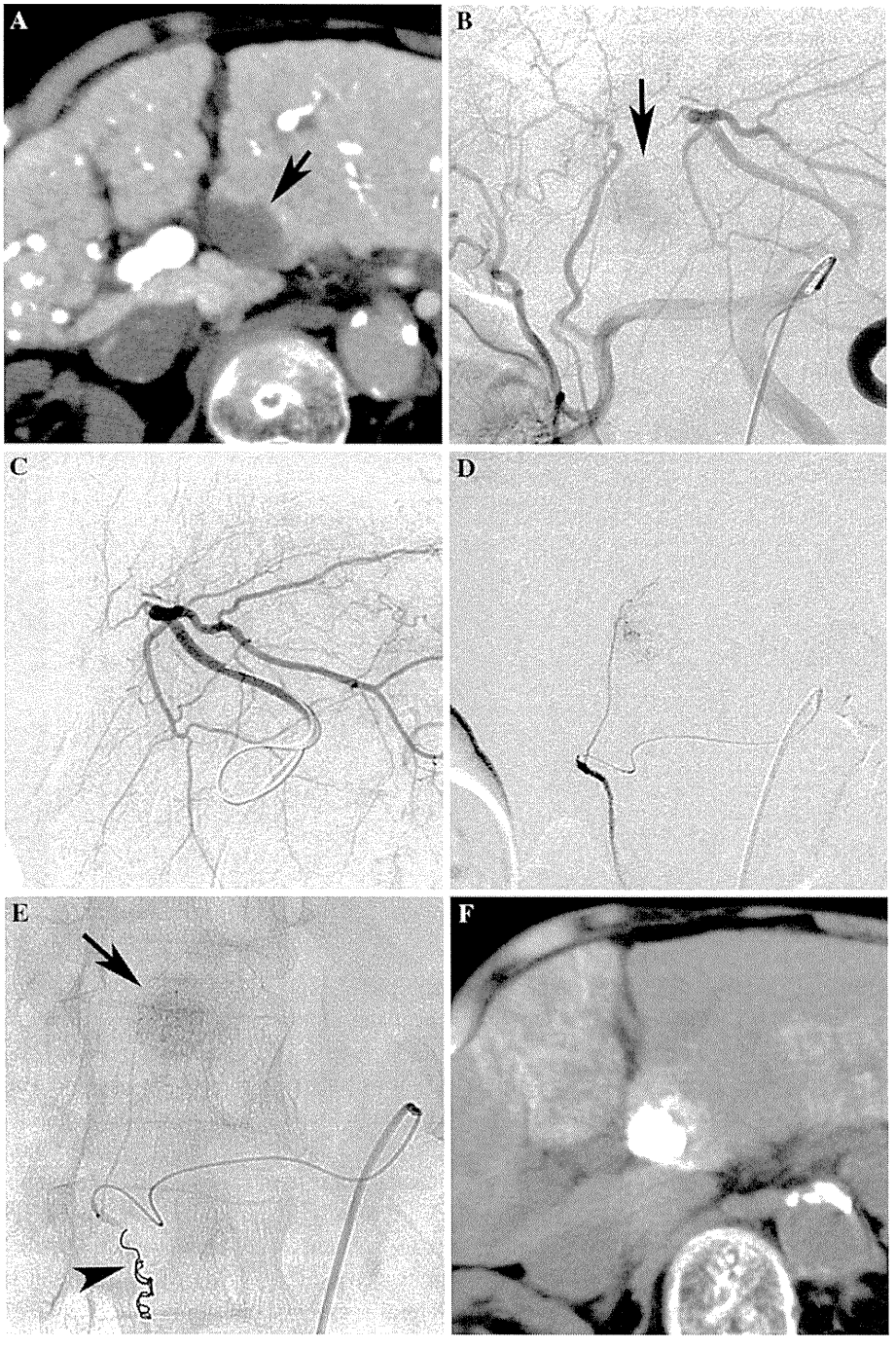


**Fig. 5** HCC located at the left side of the umbilical fissure in an 86-year-old woman. **A** CT during arterial portography revealed a tumor at the left side of the umbilical fissure (*arrow*). **B** Celiac arteriogram revealed tumor staining (*arrow*). The left lateral hepatic artery arose from the left gastric artery. **C** Left lateral hepatic arteriogram revealed no tumor staining. **D** Oblique view of an arteriogram of the right gastric artery revealed a small feeding branch. **E** The branch could not be selected, so TACE was performed after embolization of the right gastric artery with microcoils (*arrowhead*). The *arrow* indicates an iodized oil-accumulated tumor. **F** CT obtained 1 week after TACE revealed dense iodized oil accumulation in the tumor. Iodized oil was also distributed into segments 2 and 4 because additional TACE was subsequently performed on other tumors (not shown)

incidences of crossover blood supply in the present study may not reflect the natural anatomic conditions because HCC lesions usually tend to parasitize the neighboring arteries as a result of their hypervascularity. Therefore, tumor location and size might strongly influence the incidence of crossover blood supply to HCC lesions. However, we believe that our results are clinically important to appropriately select the feeding branch of tumors located near the umbilical fissure, especially when a tumor is small and its staining is faint on arteriography.

In conclusion, the present study demonstrated crossover blood supply to HCC lesions located near the umbilical fissure in addition to direct feeding from the left lateral hepatic artery or right gastric artery. When the crossover blood supply was present, the first branch of the opposite subsegmental artery fed the tumor. We think that our

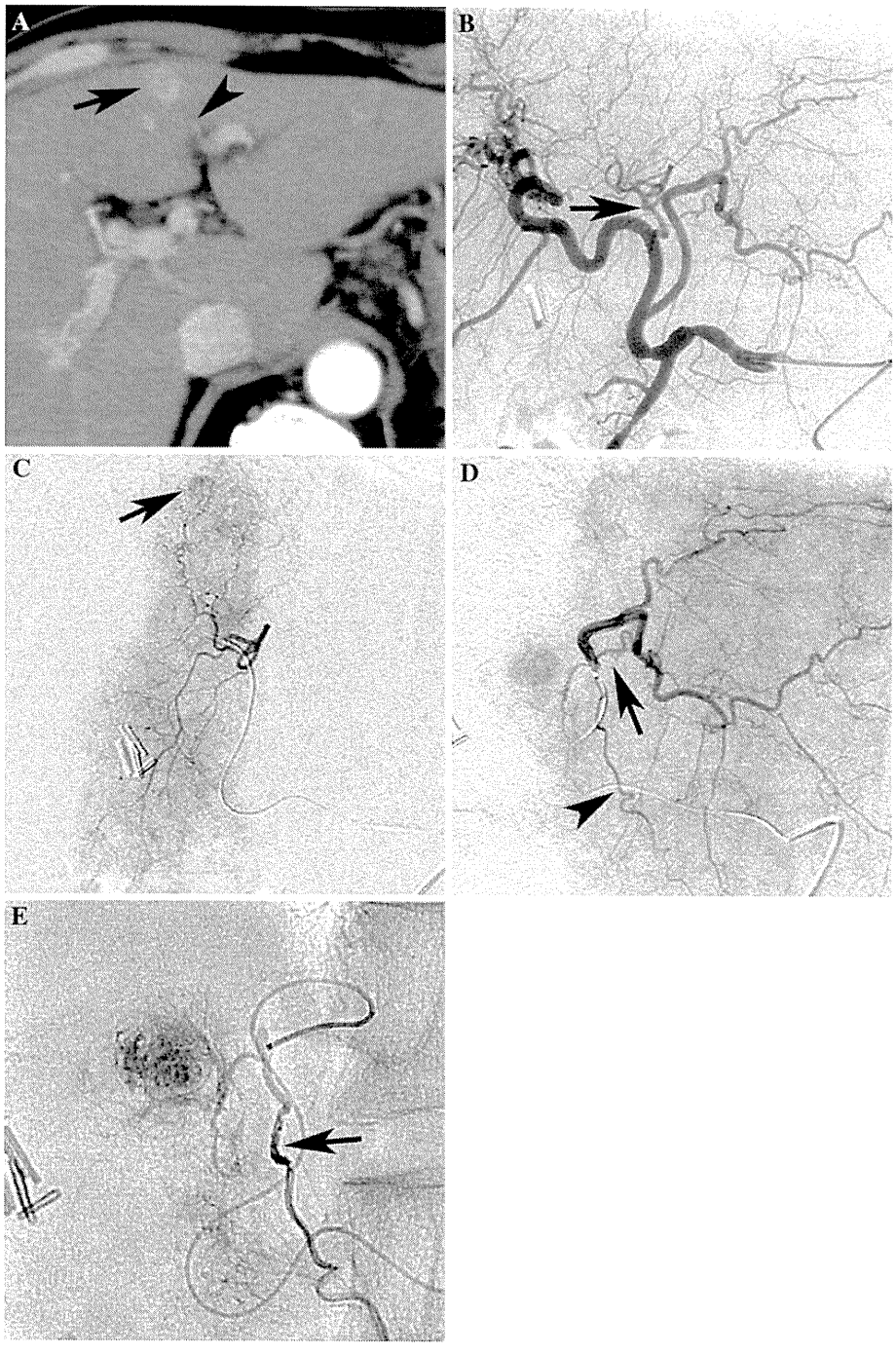


**Fig. 6** HCC located at the right side of the umbilical fissure in a 58-year-old man. **A** CT revealed a tumor (*arrow*) at the right side of the umbilical fissure (*arrowhead*). **B** Common hepatic arteriogram revealed that A4 arose as the middle hepatic artery (*arrow*). **C** Middle hepatic arteriogram revealed no obvious staining corresponded to the tumor near the umbilical fissure. A small tumor was demonstrated at another site (*arrow*). **D** Lateral left hepatic arteriogram revealed tumor staining supplied by the first branch of A3. The falciform artery also arose from this branch (*arrowhead*). **E** TACE was performed after embolization of the falciform artery with microcoils (*arrow*)

results are important to perform effective TACE for HCC lesions located near the umbilical fissure.

**Conflict of interest** The authors declare that they have no conflict of interest.

## References

1. Yamada R, Sato M, Kawabata M et al (1983) Hepatic artery embolization in 120 patients with unresectable hepatoma. Radiology 148:397–401
2. Uchida H, Ohishi H, Matsuo N et al (1990) Transcatheter hepatic segmental arterial embolization using lipiodol mixed with an anticancer drug and Gelfoam particles for hepatocellular carcinoma. Cardiovasc Intervent Radiol 13:140–145
3. Matsui O, Kadoya M, Yoshikawa J et al (1993) Small hepatocellular carcinoma: treatment with subsegmental transcatheter arterial embolization. Radiology 188:79–83
4. Miyayama S, Matsui O, Yamashiro M et al (2007) Ultraselective transcatheter arterial chemoembolization with a 2-F tip microcatheter for small hepatocellular carcinomas: relationship between local tumor recurrence and visualization of the portal vein with iodized oil. J Vasc Interv Radiol 18:365–376

5. Couinaud C (1954) Lobes et segments hépatiques: notes sur l'architecture anatomique et chirurgicale du foie. Presse Med 62:709–712
6. Bismuth H (1982) Surgical anatomy and anatomical surgery of the liver. World J Surg 6:3–9
7. Gupta SC, Gupta CD, Arora AK (1977) Subsegmentation of the human liver. J Anat 124:413–423
8. Reichert PR, Renz JF, D'Albuquerque LAC et al (2000) Surgical anatomy of the left lateral segment as applied to living-donor and split-liver transplantation: a clinicopathologic study. Ann Surg 232:658–664
9. Renz JF, Reichert PR, Emond JC (2000) Biliary anatomy as applied to pediatric living donor as split-liver transplantation. Liver Transplant 6:801–804
10. Cho A, Gunji H, Koike N et al (2007) Intersegmental arterial communication between the medial and left lateral segments of the liver. Dig Surg 24:328–330
11. Chen RC, Chou CT, Chen WT et al (2011) Delineation of the watershed between right and left hepatic arterial territories with carbon dioxide-enhanced ultrasonography. J Vasc Interv Radiol 22:667–672
12. Takeda T, Ido K, Yuasa Y et al (1988) Intraarterial digital subtraction angiography with carbon dioxide: superior detectability of arteriovenous shunting. Cardiovasc Intervent Radiol 11:101–107

Jpn J Radiol
DOI 10.1007/s11604-011-0007-x

ORIGINAL ARTICLE

# Arterial blood supply to the caudate lobe of the liver from the proximal branches of the right inferior phrenic artery in patients with recurrent hepatocellular carcinoma after chemoembolization

**Shiro Miyayama · Masashi Yamashiro · Yoshihiro Shibata · Masahiro Hashimoto · Miki Yoshida · Kazunobu Tsuji · Fumihito Toshima · Osamu Matsui**

Received: 3 May 2011 / Accepted: 31 July 2011


**Abstract**
*Purpose* To evaluate the arterial blood supply to the caudate lobe of the liver from the proximal branches of the right inferior phrenic artery (RIPA) in patients with recurrent hepatocellular carcinoma after transcatheter arterial chemoembolization (TACE).
*Materials and methods* Thirteen patients, including 10 who had a history of TACE of the caudate artery (A1), underwent TACE of the proximal RIPA branches. Iodized oil distribution was evaluated by computed tomography (CT) 1-week after TACE. Angiographic findings were also evaluated.
*Results* Previously embolized A1 was occluded ($n = 15$) or attenuated ($n = 2$). In one of three patients without A1 TACE, A1 was also attenuated. TACE was performed at the first branch of the proximal RIPA ($n = 8$), the first branch of the anterior branch ($n = 6$), and the first branch of the posterior branch ($n = 1$), respectively. Iodized oil was mainly distributed into the dorsal part of the Siegel lobe (SP) ($n = 10$), the caudate process ($n = 1$), and both ($n = 2$). In three of seven patients who had undergone serial RIPA angiography, RIPA parasitization to SP was suspected before A1 TACE.
*Conclusion* The proximal RIPA branches mainly supply the SP when A1 is attenuated.

S. Miyayama (✉) · M. Yamashiro · Y. Shibata · M. Hashimoto · M. Yoshida · K. Tsuji · F. Toshima
Department of Diagnostic Radiology, Fukuiken Saiseikai Hospital, 7-1 Funabashi, Wadanaka-cho, Fukui 918-8503, Japan
e-mail: s-miyayama@fukui.saiseikai.or.jp

O. Matsui
Department of Radiology, Kanazawa University Graduate School of Medical Science, 13-1 Takara-machi, Kanazawa 920-8641, Japan

**Keywords** Hepatocellular carcinoma · Right inferior phrenic artery · Caudate lobe

## Introduction

The inferior phrenic arteries (IPAs) are the major blood source to the diaphragm. There is close contact between the posterior portion of the liver and the diaphragm at the bare area, and branches of the right IPA (RIPA) are in direct contact with the liver [1–3]. Therefore, the RIPA is the most common extrahepatic collateral vessel supplying hepatocellular carcinoma (HCC) [4, 5].

The caudate lobe of the liver is located at the bare area; consequently, several extrahepatic collateral vessels directly enter into the caudate lobe at this location. The RIPA also enters into the caudate lobe and supplies HCC lesions, particularly when the tumor recurs after transcatheter arterial chemoembolization (TACE) [6, 7]. Several branches are derived from the RIPA [1, 2, 8], and it is clinically important to determine which branches of the RIPA have a potential to reach the caudate lobe and supply the tumor.

The purpose of this study was to evaluate the arterial blood supply to the caudate lobe of the liver from the proximal branches of the RIPA using angiograms and computed tomographic (CT) images obtained during and after TACE for locally or distantly recurrent HCC located in or near the caudate lobe.

## Materials and methods

This was a retrospective study in which the arterial blood supply to the caudate lobe of the liver from the proximal branches of the RIPA was evaluated using imaging data and

Published online: 03 December 2011

clinical records with no change in patient care. Institutional review board approval is not required at our institution for this type of study. Written informed consent was obtained from each patient before the TACE procedure.

### Selection criteria

Blood supply to the caudate lobe from the RIPA was evaluated by the distribution of iodized oil injected during selective TACE through the proximal branches of the RIPA facilitated by CT imaging. We excluded patients who underwent non-selective TACE of the RIPA, patients who had an obvious anastomosis between the caudate artery and the RIPA on angiography, and patients who underwent TACE through both the caudate artery or neighboring hepatic branches and the branch of the RIPA in a single procedure. We also excluded patients who had HCCs of >3 cm in diameter in the caudate lobe protruding from the liver because the parasitic blood supply is exaggerated in such cases.

### Patients

Between April 2002 and January 2011, we identified 13 patients (8 men, 5 women) who met the above selection criteria. The mean patient age [±standard deviation (SD)] was 69.2 ± 9.1 years (range 49–82 years). All patients had liver cirrhosis which was associated with hepatitis C in 10 patients, hepatitis B in two patients, and of unknown etiology in one patient. All patients had previously undergone 1–11 TACE sessions (4.5 ± 3.4 times). Ten patients had previously undergone one to two selective TACE sessions (1.6 ± 0.5 times) of the caudate artery for a tumor in ($n = 9$) or adjacent to the caudate lobe ($n = 1$). Three patients also had undergone radiofrequency ablation for a tumor beside the caudate lobe.

The diagnosis of HCC was established by findings on CT and/or magnetic resonance imaging scans, such as characteristic nodular enhancement on arterial phase images and wash-out on delayed phase images, in addition to nodular staining on angiography and/or CT images during hepatic arteriography (CTHA) and nodular perfusion defect on CT images during arterial portography (CTAP) obtained using CT or cone-beam CT (CBCT).

In all patients, unenhanced CT was obtained 1 week after TACE in order to check for iodized oil distribution. In addition, blood supply to the caudate lobe from the RIPA was confirmed in four patients using CT ($n = 1$) or CBCT ($n = 3$) during the TACE procedure.

### TACE procedure

All TACE procedures through the hepatic artery and RIPA were performed by injecting either a mixture of 2–5 ml of iodized oil (Lipiodol; Andre Guerbet, Aulnaysous-Bois, France) and anticancer drugs [10–30 mg of epirubicin (Farmorbicin; Pfizer, Tokyo, Japan) and 2–4 mg of mitomycin C (Mitomycin; Kyowa Hakko Kirin, Tokyo, Japan)] followed by gelatin sponge particles (Gelfoam; Upjohn, Kalamazoo, MI or Gelpart; Nippon Kayaku, Tokyo, Japan). A 1.8-F tip (Carnelian PIXIE; Tokai Medical Products, Kasugai, Japan), 2-F tip (Progreat α; Terumo, Tokyo, Japan), and 2.4-F tip (Microferret; Cook, Bloomington, IN) were navigated to the tumor-feeding branch using a 0.016-inch guide wire (GT-wire; Terumo) through a 4-F catheter. TACE of the RIPA was performed as selectively as possible through a microcatheter advanced into the small branch.

### Assessment

Iodized oil distribution to the caudate lobe in all patients was evaluated by unenhanced CT performed 1 week after TACE, and the condition of the previously embolized caudate artery was evaluated by angiography. CT or CBCT during angiography of the RIPA or its branch was also evaluated. The caudate lobe can be divided into three subsegments according to the classification proposed by Kumon [9], namely, the Spiegel lobe (SP), the paracaval portion (PC), and the caudate process (CP); the distribution of iodized oil (partial or complete) was also evaluated in each of these subsegments of the caudate lobe (Fig. 1).

When angiography of the RIPA had been performed during the previous TACE procedures, those findings were retrospectively evaluated and compared.

## Results

A summary of the clinical data on each patient is shown in Table 1.

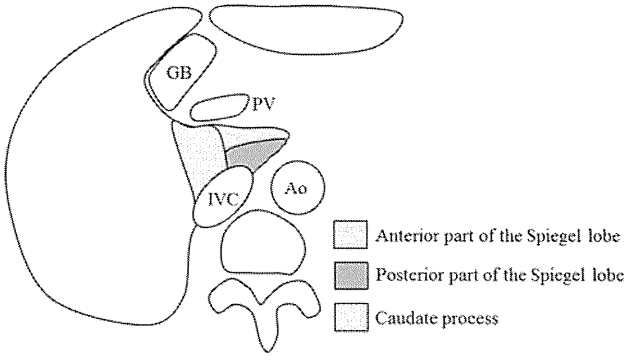


*GB* gallbladder, *PV* portal vein, *IVC* inferior vena cava, *Ao* aorta

**Fig. 1** Schematic presentation of the Spiegel lobe and caudate process of the caudate lobe of the liver